Boulder fall activity in the Jezero crater, Mars

Rishitosh K Sinha, A. Rani, Susan J. Conway, S. Vijayan, A. Basu Sarbadhikari, M. Massé, N. Mangold, A. Bhardwaj

Boulder fall activity in the Jezero crater, Mars

R. K. Sinha[1], A. Rani[1], S. J. Conway[2], S. Vijayan[1], A. Basu Sarbadhikari[1], M.Massé[2], N. Mangold[2], A. Bhardwaj[1]

[1]Planetary Sciences Division, Physical Research Laboratory, Ahmedabad 380009, India.

[2]CNRS, UMR 6112 Laboratoire de Planétologie et Géodynamique, Université de Nantes, Université d'Angers, France.

Corresponding author: Rishitosh K. Sinha (rishisrmice@gmail.com)

Key Points:

- We report on previously unrecognized boulder fall activity in Jezero crater – landing site of Mars 2020 Perseverance rover
- Hazardous boulders bigger (length >2.7 m) than the rover have recently fallen on the front of the western delta deposits within the crater
- Recently fallen boulders may have freshly exposed surfaces, which can be ideal targets for astrobiological investigations by the rover

Abstract

Jezero crater is the landing site for the Mars 2020 Perseverance rover. We report 63 boulder fall tracks within the crater using High Resolution Imaging Science Experiment (HiRISE) images. The boulder tracks have both fresh and faded morphologies similar to those reported elsewhere on Mars, but reported for the first time in Jezero crater. We combine observations from 16 boulder-tracks on the western delta deposit with 47 in the surrounding regions to infer possible process(es) of boulder destabilization, which can be tested with rover observations. This newly-found hazard should be taken into account for rover operations. Boulders associated with tracks are geologically "recent falls", so it is possible that the surfaces of these boulders may provide an opportunity to sample material less exposed to radiation than other rocks at the martian surface and could be ideal targets to analyze for organics.

Plain language summary

We have found tracks left by falling boulders within Jezero crater on Mars, which is the landing site of the Mars 2020 Perseverance rover. The boulder tracks are observed on the slopes of the delta deposits that the rover will explore, on the wall of Jezero crater and on the wall of a ~2km diameter crater on the floor of Jezero crater. Boulders of a few meters in size have fallen down moderately steep slopes, moving distances from a few tens of meters to nearly a kilometer. The boulder tracks appear both fresh and degraded. The positions of the boulders and the appearance of the tracks have not been observed to change, but the simple existence of the tracks suggests that the boulder falls are recent and could be ongoing. Our results reveal a new location on Mars where boulder fall activity is observed and indicate a new hazard to be taken into account by the rover team. These recently fallen boulders may also have surfaces less exposed to radiation and could

be ideal candidates for obtaining samples that could be analyzed for signs of ancient life. Such signs usually degrade rapidly with exposure to radiation.

1 Introduction

Boulder falls are energetic events and are known to occur on Mars **(e.g. Roberts et al., 2012; Brown and Roberts, 2019; Kumar et al., 2019)**. Hence, understanding if such a process could occur within the landing site of a roving mission on Mars is a key factor when planning operations to ensure the safety of the rover **(e.g. Golombek and Rapp, 1997; Golombek et al., 2003, 2008, 2012)**. Recent boulder falls are characterized by a track marked in the regolith in the wake of the boulder. The tracks are continuous and/or discontinuous depressions of a similar width to that of the boulder with slightly raised edges and are produced by rolling, bouncing and rotation of the boulders **(van der Bogert and Plescia, 2014)**. Over time, the boulder tracks may be erased by the deposition of dust **(Beyer, 2012**), infilling by aeolian deposits, and/or aeolian abrasion.

Isolated boulders are often key science targets for roving missions, as they are more easily accessible than outcrops and they can reveal information both on the mineralogy and geochemistry of the surface **(e.g. Morris et al., 2000; Hamilton and Ruff, 2012; Squyres et al., 2006; Stolper et al., 2013; Pajola et al., 2017; Wiens et al., 2020)**. Boulders with tracks have the additional advantage that they can be traced back to the specific source region and hence enable a roving mission to sample rocks from the locations that would generally be difficult to reach **(Schmitt and Cernan, 1973; Senthil Kumar et al., 2016)**.

The landing site of the Mars 2020 Perseverance rover (Jezero crater; centered at 18.42˚N, 77.67˚ E) is a proposed paleolake with two inlet channels feeding the crater from the north and west **(Figure 1a; Fassett and Head, 2005)**. The approximate position of the landing ellipse of the rover and the potential traversable routes of the rover to regions of interest within the landing site surrounds the partially eroded delta deposits (also known as western delta deposit) at the mouth of the western inlet channel **(Figure 1b; Fassett and Head, 2005; Goudge et al., 2015, 2017; Farley, 2018; Mangold et al., 2020; Williams et al., 2020)**. Presence of aeolian landforms such as yardangs and transverse aeolian ridges (TARs) has been reported over the volcanic deposits on the front of the delta deposits **(Chojnacki et al., 2018; Day and Dorn, 2019)**, and aeolian erosion has been suggested to have extensively eroded the delta deposits **(Fassett and Head, 2005; Schon et al., 2012)**. In addition, the front of ~50-60 m high western delta deposit hosts numerous boulders on its top surface, over its talus slope and at the base of the talus slope. Numerous boulders are found scattered across the wall of Jezero crater. If a boulder has detached from the face of the delta front or the crater wall in the very recent past at geological time scales, it is likely that the boulder would have produced a track as it rolled/bounced over the slope materials under the force of gravity. To our knowledge, boulder fall activity within Jezero crater has never been examined in detail. In this study we used 13 Mars Reconnaissance Orbiter (MRO) HiRISE images (0.25 or 0.5 m/pixel) and 4 HiRISE stereo-pair derived digital terrain models (DTM) (1 m grid spacing) **(McEwen et al., 2007; Kirk et al., 2008) (Table S1 and S2, Figure S7)** to search for boulder fall tracks, and analyze the morphology of identified boulder tracks. We examined all slopes for boulder tracks, including the flanks of delta deposits, Jezero crater wall, the walls of any other craters on the floor of Jezero, on the flanks of mounds adjacent to the Jezero crater wall, and on the flanks of any other topographic or hill-like features on the Jezero crater floor. To test whether boulder falls are currently active, we examined images with a long time separation **(Table S3)** to seek signs of change in the boulder position and the boulder track morphology (for example, fading of boulder tracks). We used the empirical shadow angle method **(Lied, 1977; Evans and Hungr,**

1993) to analyze the runout distance of boulder falls on the delta deposits. Shadow angle is the angle between the horizontal line from the talus apex and the line that connects the talus slope apex with the most distant boulder fall **(Duszynski et al., 2015)**. Please see the supporting information for details on the data and methods. Finally, we discuss the possible process of boulder destabilization and explore the potential scientific implications for the Mars 2020 Perseverance rover.

2 Results

We have identified 63 boulder tracks within Jezero crater **(Dataset S1)**. 16 boulder tracks are on the front of western delta deposits and the remaining 47 boulder tracks are in other regions of the crater (43 boulder tracks on/near the wall of Jezero crater and 4 boulder tracks on the wall of a ~2 km crater on the floor of Jezero crater) **(Figure 1b-1d)**. We did not identify any convincing changes in the position of the boulders and tracks have not faded over the ~12 years of available images **(Figure S1) (Table S3)**. We found that the tracks reported in this study do not appear/disappear with respect to the change in the illumination conditions (such as incidence angle and subsolar azimuth) (Table S1).

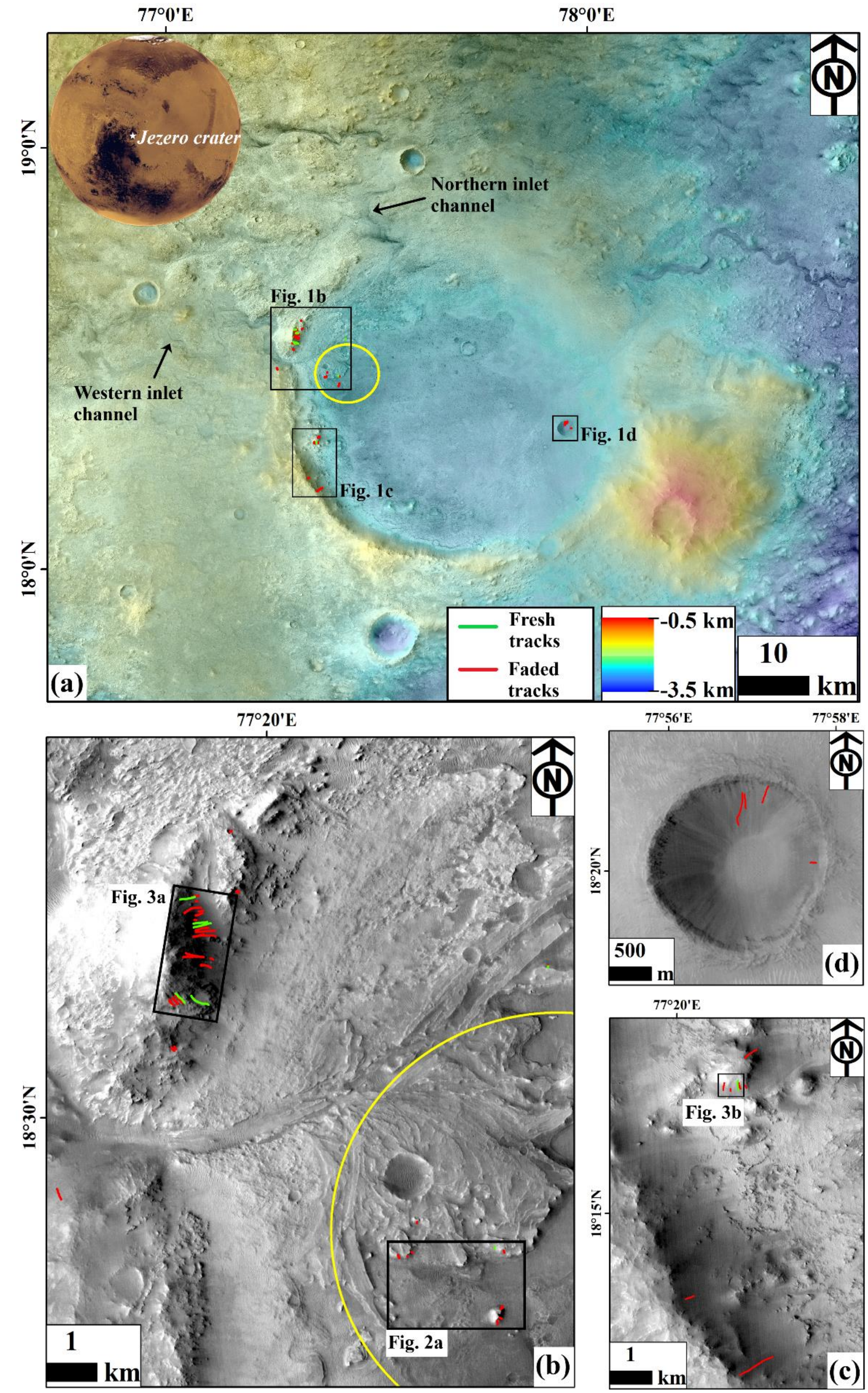
77°0'E
78°0'E
19°0'N
18°0'N
*Jezero crater
Northern inlet channel
Western inlet channel
Fig. 1b
Fig. 1c
Fig. 1d
Fresh tracks
Faded tracks
-0.5 km
-3.5 km
10 km
(a)
77°20'E
18°30'N
Fig. 3a
Fig. 2a
1 km
(b)
77°56'E
77°58'E
18°20'N
500 m
(d)
77°20'E
18°15'N
Fig. 3b
1 km
(c)
N

Figure 1. (a) Mars Orbiter Laser Altimeter (MOLA) and High Resolution Stereo Camera (HRSC) blend color elevation map over the Context (CTX) camera mosaic of the region around Jezero crater (Dickson et al., 2018). The location of Jezero crater (star) is shown on the global view of Mars (top-left) using Viking color imagery. The locations of panels b-d are shown by black boxes. The Mars 2020 Perseverance rover landing ellipse is in yellow. (b) Boulder fall tracks identified on the western delta deposits and western wall. (c) Additional boulder tracks identified on the western wall. (d) Boulder tracks identified on the wall of a ~2 km crater on the floor of Jezero crater. Background is CTX mosaic in panels b-d. CTX image mosaic credits: NASA/JPL/MSSS/Caltech Bruce Murray Lab.

2.1 Boulder falls on the western delta deposits

We have identified 14 faded and 2 fresh boulder tracks on the front of western delta deposits **(Figures 1b, 2a)**. The morphology of faded boulder tracks varies widely between the tracks **(Figure 2b-d)**. For five of the faded boulder tracks, depressions are still identifiable, but for the 9 other faded boulder tracks only the track margin is discernible. We interpret this difference in boulder track morphology to be related to the extent to which they are mantled by dust, and therefore could give us an indication of the relative ages of the tracks. Fresh boulder tracks are characterized by distinct depressions **(Figure 2e)**.

In general, all the boulder tracks end on the talus slope with an average length of 31 m **(Figures 2b-c, 2e, 2g)**. The boulders associated with the tracks measure <4 m in length (mean: 1.7 m, standard deviation: 0.8 m) **(Figure 2f)**. Widths of boulder tracks vary from 1 m to 3.3 m (mean: 1.8 m, standard deviation: 0.7 m) **(Figure 2f)**. The average slope between the start and end of the tracks ranged from 16˚ to 29˚ with most between 17˚ and 24˚ (mean: 22˚, standard deviation: 3.8˚) **(Figure 2h)**. The longest observed boulder track (67 m) is associated with a big boulder (length: 3.7 m) that has travelled beyond the base of talus slope, and the track superimposes aeolian landforms (e.g. TARs/dunes) **(Figure 2d)**. Compared to the other fallen boulders around the delta deposits, this big boulder is double their average length (1.7 m). In comparison to the 63 boulder falls reported in this study, this big boulder is nearly 3 times their average length (1.3 m). Both longer (44 m to 67 m) and shorter (16 m to 30 m) boulder tracks have an average slope between 16˚ and 21˚. The average slope of the boulder source regions varies from 5˚ to 47˚ (mean: 23˚, standard deviation: 13.6˚) **(Figure 2h)**.

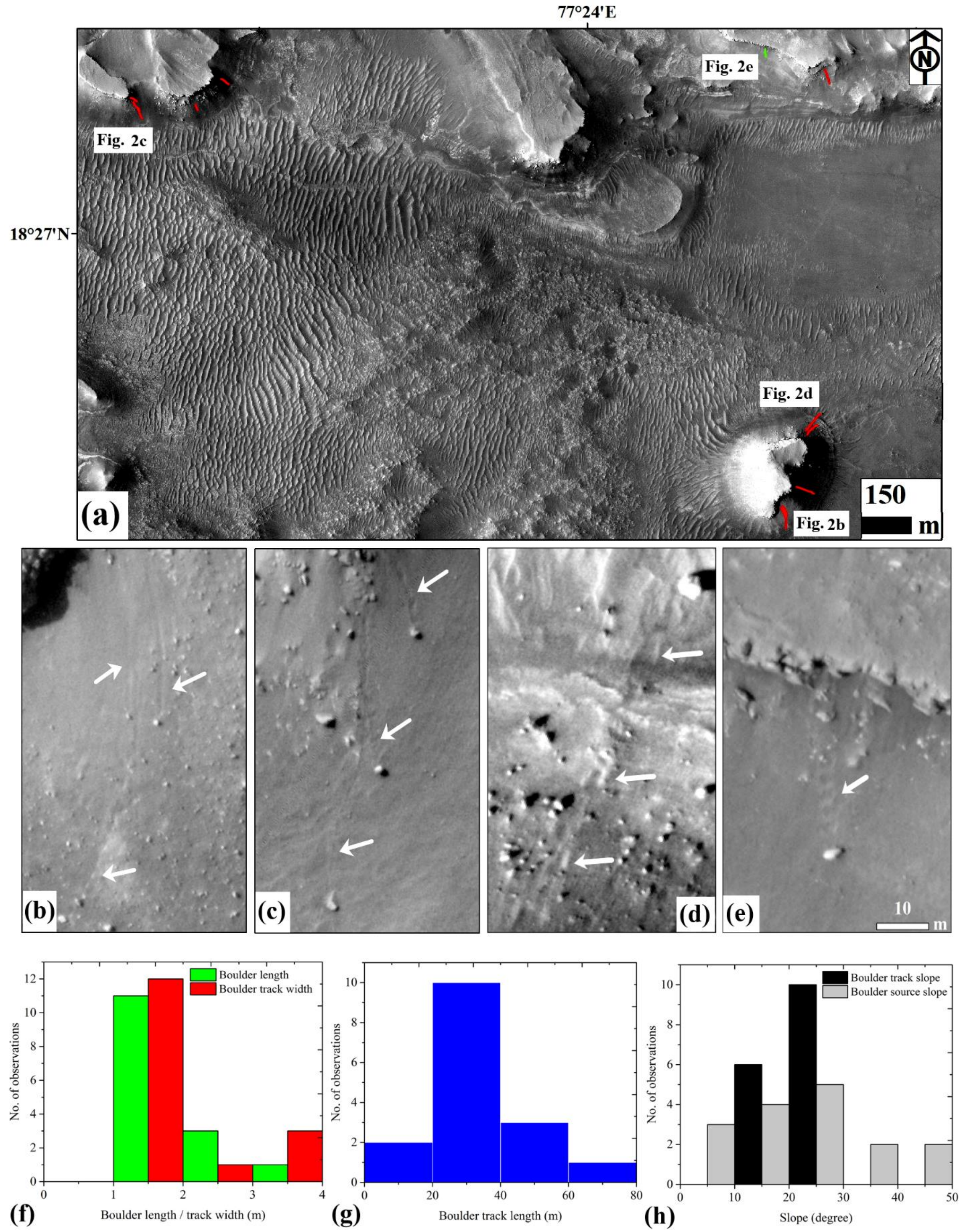

77°24'E
18°27'N
Fig. 2c
Fig. 2e
Fig. 2d
Fig. 2b
150 m
(a)
(b)
(c)
(d)
(e)
10 m
Boulder length
Boulder track width
No. of observations
Boulder length / track width (m)
(f)
Boulder track length (m)
(g)
Boulder track slope
Boulder source slope
Slope (degree)
(h)

163

Figure 2. (a) Overview of the front of western delta deposits within Jezero crater on which fresh (green) and faded (red) boulder fall tracks are found. Locations of panels 2b-e are labeled. (b-d) Detailed view of faded boulder tracks (arrows). In Figure 2d, a custom stretch was applied to enhance contrast of the boulder track. (e) Detailed view of a fresh boulder track (arrow). Scale is same in panels b-e. HiRISE Image ID (a-e): PSP_002387_1985, credits: NASA/JPL/University of Arizona. (f-h) Morphometric characteristics of boulder fall on the front of western delta deposits. Histograms of (f) boulder length and boulder track width, (g) boulder track length, (h) boulder track slope and boulder source slope. The measured values plotted in f-h are rounded to 1 decimal place.

2.2 Boulder falls in the other regions of the crater

40 boulder tracks out of the 47 observed tracks **(Figures 1b-d** and **3a-b;** 36 tracks on/near the Jezero crater wall and 4 tracks on the wall of a ~2 km crater on the Jezero crater floor) are classified as faded tracks **(Figures 3f-g and 3i)**. The remaining 7 boulder tracks (on/near the Jezero crater wall) have a fresh morphology **(Figures 3c-e and 3h)**. The faded tracks lack identifiable depressions, and appear infilled or mantled by dust, whereas the fresh tracks are characterized by distinct depressions. The boulders observed here (mean size: 1.2 m, standard deviation: 0.6 m) have formed tracks of length and width in the range 33 m – 900 m (mean: 190 m, standard deviation: 155 m) and 0.5 – 2.6 m (mean: 0.9 m, standard deviation: 0.5 m), respectively. The slope of the boulder source regions is slightly steeper (mean: 24°, standard deviation: 4°) than the slope of the boulder tracks (mean: 20°, standard deviation: 2.1°).

We find that the orientation of the slopes on which the boulder tracks are found are preferentially: (1) southeast **(Figure 3m)**, (2) east-southeast **(Figure 3n)**, and (3) west-southwest/east-northeast **(Figure 3o)**.

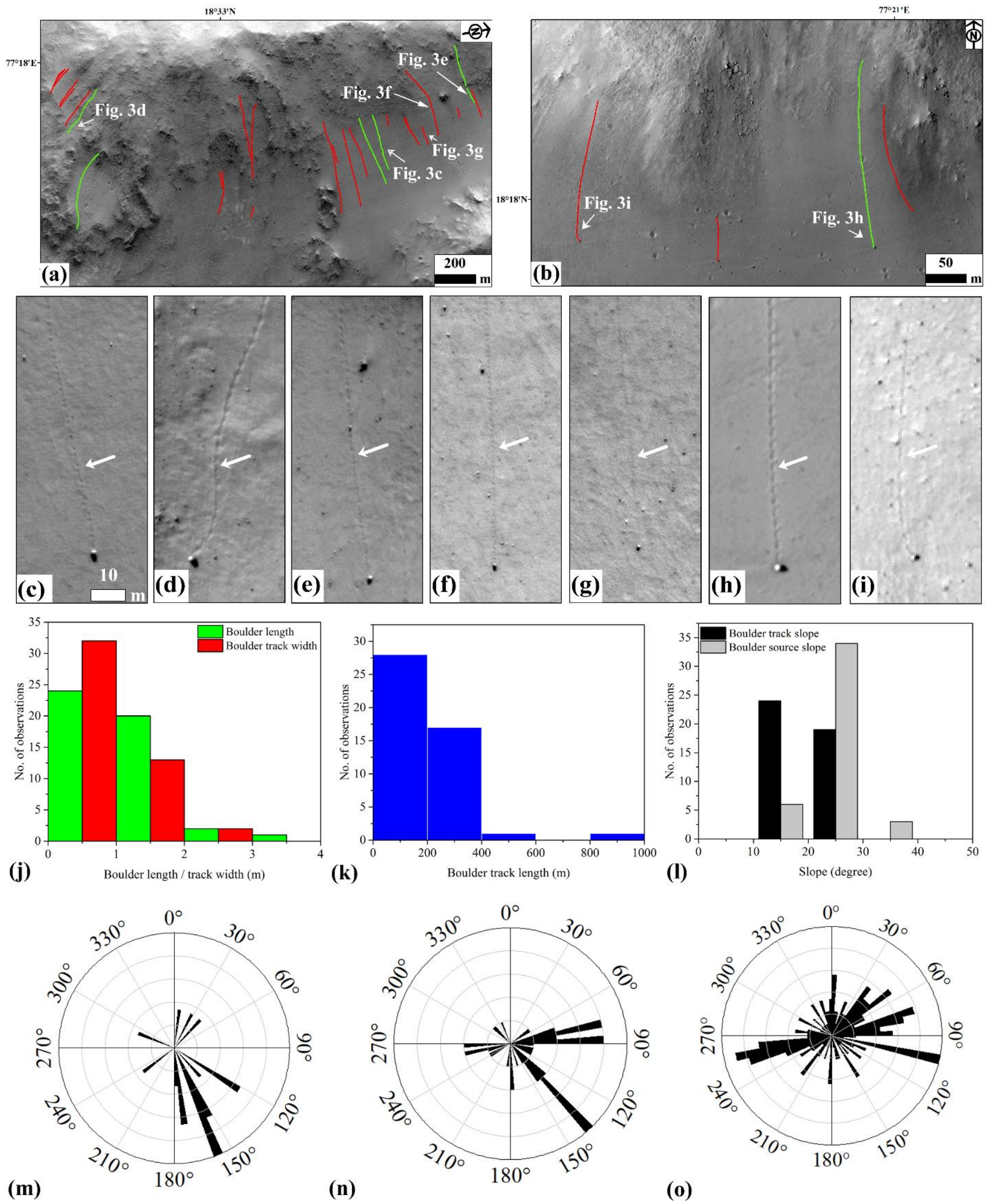

Figure 3. (a-b) Overview of the fresh (green) and faded (red) boulder tracks newly identified on/near the wall of Jezero crater. HiRISE Image ID (a): ESP_037119_1985. HiRISE Image ID (b): PSP_001820_1985. Locations of panels 4c-i are shown. (c-e): Detailed views of example

faded boulder tracks (arrows). (f-i): Detailed views of example fresh boulder tracks (arrows). Scale is same in panels c-i. HiRISE Image credits: NASA/JPL/University of Arizona. (j-l) Morphometric characteristics of the boulder falls on/near the wall of Jezero crater. Histograms of (j) boulder length and boulder track width, (k) boulder track length, (l) boulder track slope and boulder source slope. The measured values plotted in j-l are rounded to 1 decimal place. Orientation of slopes on which the boulder fall tracks are observed on (m) delta deposits, (n) crater wall, and (o) the walls of 6 small craters (diameter: ~1.5 – 5 km) located within two to three crater radii of Jezero crater **(Figure S2, S8)**.

2.3 Boulder runout distance and shadow angle

Runout characteristics of the boulders fallen around the delta deposits is inferred from the ratio between the horizontal distance travelled by the boulder (L) and the vertical fall height (H) of the boulder. The L/H ratios for boulder falls on the delta deposits is greater than ~1.6 with a mean value of 2.5 **(Figure 4a)**. The correlation coefficient for best-fit is 0.75 using a linear regression function. We find that on the delta deposits, both smaller (≤1-1.2 m) and bigger (3.7 m) boulders have L/H ratio ≥3, suggesting that boulder size is not the primary driver for runout distance on the delta deposits. The shadow angle is estimated as the arctangent of the relationship between the vertical drop of the boulder (elevation difference between the apex of talus slope and final elevation of the fallen boulder) and the horizontal distance travelled by the boulder (distance between the apex of the talus slope and final location of the fallen boulder). The shadow angle ranges between 16.2° and 27.1° for boulder falls on the delta deposits **(Figure S3)**. On the front of delta deposits, the increase in runout distance (67 m) and reduction in minimum shadow angle (16.2°) resulted in boulder runout beyond the base of talus slope. This is consistent with the observational evidence that the runout of the boulders on the talus slope was not influenced by the aeolian landforms on the front of delta deposits. The mobility of the boulders that we have calculated (using the shadow angle) is within the range of those calculated for terrestrial rock falls **(Evans and Hungr, 1993; Copons et al., 2009)**. Hence, there cannot be a significant acceleration (or addition of energy) above that of simply gravity acting alone. No trend is identifiable in the plot of boulder fall size (m^3) versus tangent of the shadow angle **(Figure 4c)**.

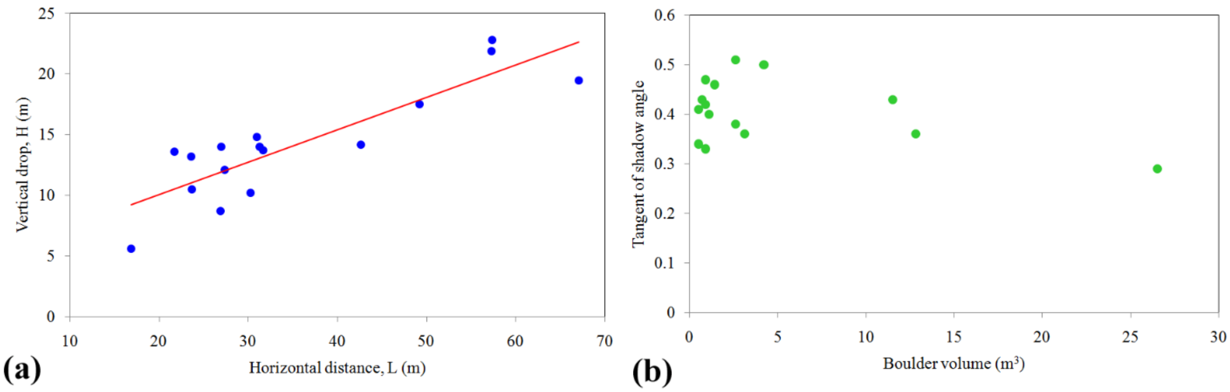

Figure 4. (a) Plot of horizontal distance (L) versus vertical drop (H) with fitted linear regression lines for delta deposits ($R^2 = 0.75$). (**b**) Plot of boulder volume (volume of individual boulders in m^3) versus tangent of the shadow angle for boulders with tracks sourced at the delta deposits.

3 Discussion

We report previously undetected boulder fall activity at the landing site of Mars 2020 Perseverance rover. The average slopes (22° for the delta front and 20° for the other regions of the crater) onto which the boulders have fallen are lower than the angle of repose (30°) for dry particles on Mars **(Kleinhans et al., 2011; Atwood-Stone and McEwen, 2013)**. Some (3 of the 16 boulders with tracks on the western delta deposits) of the boulders that have moved (length >2.7 m) are bigger than the Mars 2020 Perseverance rover (width 2.7 m, and height 2.2 m) **(Figure S4)**. The proposed traverse of the Perseverance rover is along the front of delta deposits; therefore, it is important to understand the processes of boulder destabilization and whether it could still be ongoing today, which we will discuss further below.

3.1 Process of boulder destabilization

Evidence of frost has been reported at low latitudes on Mars (15-30˚) **(Schorghofer and Edgett, 2006; Carozzo et al., 2009; Vincendon et al., 2010a, 2010b)** and at the Opportunity rover landing site (at 1.95˚ S) **(Landis, 2007)**. If seasonal frosts also occur at Jezero crater, the rocks therein could be broken down by the stress produced due to volume change of frost condensed in cracks. Seasonal and diurnal temperature differences at latitudes poleward of 20-30˚ are estimated to develop tensile stress >2-3 MPa in ice cemented ground **(Mellon, 1997)**. However, whether thin frosts in fractured rocks at equatorial latitudes can induce such thermal contraction cracks is unknown but is a factor to consider for breaking down and destabilizing boulders in Jezero crater.

Solar insolation induced thermal stress has been proposed as a mechanism for rock breakdown on the surface of Mars **(Eppes et al., 2015),** and has been shown to lead to rock falls with preferential orientations (**Tesson et al., 2020**). However, we find that the boulder tracks do not exhibit any similarity in the preferred orientations **(Figure 3m-o)**. So although thermal stresses probably contribute to rock breakdown, they do not seem to be the principal driver for destabilization.

Wind could scour beneath boulders causing them to fall **(e.g., Malin and Edgett, 2001)**. Aeolian bedforms indicate modern easterly winds in the interior of Jezero crater **(Chojnacki et al., 2018; Day and Dorn, 2019)** and Jezero crater is located in a high sand flux region of Mars **(Chojnacki et al., 2018)**. Previous studies have implicated aeolian erosion for the erosion of delta deposit within the crater **(Fassett and Head, 2005; Schon et al., 2012; Day and Dorn, 2019)** and a less erosion-resistant rock layer is known to be removed by aeolian scour and induce scarp retreat in Jezero crater **(Williams et al., 2020)**. Hence, aeolian processes seem a likely driver for boulder destabilization in Jezero crater.

Lithological differences can favor boulder destabilization. Mass wasting (in form of boulder falls and movement of the boulders) of the sulfate-rich sediments in the equatorial region of Mars is 3-4 orders faster than the average erosion rate on the martian surface **(Thomas et al., 2019)**. Mineralogical mapping of the delta front where we have observed boulder falls indicates the presence of Fe/Mg smectites **(Goudge et al., 2017),** but fresh boulder tracks are not confined to this unit **(Figure 1b)**, and various minerals have been reported in these regions **(Goudge et al., 2015, 2017)**. Hence, we do not find a specific role for lithology in explaining the boulder falls in Jezero crater.

Boulders can be mobilized downslope by the ground shaking caused by meteorite impacts or seismic shaking. We found no fresh impact craters within two to three crater radii of Jezero crater. We found boulder fall tracks within Jezero crater as well as on the wall of 6 small craters distributed within a radial distance of 60-70 km around the Jezero crater (two to three crater radii) **(Figure S2, S8)**. We have not observed any recent impact crater within this 60-70 km radius around Jezero crater to account for impact causing shaking in the study region. Previous work has found that boulder falls resulting from seismic shaking can be observed over a distance of several kilometers from visible surface faulting (for example in Cerberus Fossae) **(Roberts et al., 2012)**. Jezero crater is close to a group of large, concentric grabens, called Nili Fossae, although there have been no reports of these faults being active on geologically recent timescales. A detailed examination of the HiRISE images of the Nili Fossae would be needed to understand if recent mobilization of boulders has occurred systematically along the strike of the faults in the region, which is beyond the scope of this paper. Hence, we maintain that seismic shaking is a plausible hypothesis for boulder mobilization at this location, but have no corroborating evidence. A previous study reported a paleomarsquake of moment magnitude 'M_w' up to 7.3-7.8 from boulder track data in Grjota Valles **(Brown and Roberts, 2018)**, but InSight (Interior exploration using Seismic Investigations, Geodesy and Heat Transport) instruments have only observed marsquakes, 'M_w' <4 **(Banerdt et al., 2020)**. Therefore, detailed modeling would be needed to understand the proximity and magnitude of seismic events to mobilize boulders as large as 3.7 m at Jezero crater.

The data presented here are not sufficient to determine the recurrence interval of boulder falls at Jezero crater; hence we cannot assess the likelihood of boulder falls happening during the Mars 2020 mission. We have observed fresh and faded tracks in close proximity **(Figures 1b-1d, 2, 3)**, suggesting that neighboring tracks have different ages (as they should share similar environments), and the processes destabilizing the boulders within Jezero crater has been active over a prolonged period. The evidence of fresh tracks on the western delta deposits, on the western wall of crater, and on the wall of small craters in the vicinity of Jezero crater suggests that the boulder destabilization process is not local and was last active relatively recently. If the boulders continued to move once the track has formed, then this motion has a magnitude less than a meter in ~12 years.

3.2 Other Implications for the Mars 2020 mission

While the process for boulder destabilization is still unclear, the hypotheses we present could be tested by the Mars 2020 Perseverance rover, scheduled to arrive in Jezero crater in early 2021. For instance, the mast-mounted camera system (MastCam-Z) has wavelength filters that could detect frost deposits **(Rice et al., 2020)**, while the Radar Imager for Mars' subsurface eXperiment (RIMFAX) would be able to identify any subsurface ice **(Russell et al., 2020)**. The onboard cameras can be used to monitor aeolian transport and abrasion and look for clues of thermal breakdown. The role of wind or frost could also be tested by the Mars Environmental Dynamics

Analyzer (MEDA), which will monitor wind speed and directions, surface temperature and measure local humidity **(de la Torre Juárez et al., 2020)**.

Our observations open the door for in-situ analyses of boulders whose source areas would ordinarily not be accessible directly by the rover. The tracks allow their provenance to be better ascertained than boulders without tracks. Some of the boulders at the foot of the delta are present on slopes as low as 4-15° **(Figure S5)**, thus accessible by a rover, and have been detached from source regions where Fe/Mg smectites are thought to be present **(Goudge et al., 2017)**. Boulders present on the foot of crater wall at slope as low as 20° **(Figures 1c, 3a-b** and **Figure S6)** could also provide access to the crater rim material, thus to ancient pieces of the crust **(e.g. Goudge et al., 2017)**. In addition boulders with tracks are geologically "recent falls", so these recently fallen boulders may provide an opportunity to drill fresh exposures which might be less exposed to radiation than other rocks at the martian surface and hence could present ideal targets to analyze for organics **(Cockell et al., 2016)**.

4 Conclusions

We demonstrate a previously unknown boulder fall activity on the talus slope of the western delta deposits and on/near the wall of Jezero crater. The relative paucity of monitoring data (time step of before-and-after images limited to ~12 years) does not allow us to conclude whether boulder fall and boulder track modification are actively occurring at the present-day or not. Nevertheless, our observations suggest boulders with visible tracks to have detached during recent geological time scales. Surfaces of these recently fallen boulders therefore present a set of potential targets for measurement of organic molecules by the Mars 2020 Perseverance rover. With the available data we cannot determine which process or processes may have been responsible for the boulder falls in and around Jezero crater, but propose hypotheses that can be tested by the rover (such as: thermal contraction, aeolian erosion, seismic shaking).

Acknowledgements

We thank the Editor (Andrew J. Dombard) and the reviewers (Mackenzie Day and Hirdy Miyamoto) for providing us with constructive comments and suggestions. The work at the Physical Research Laboratory is supported by the Indian Space Research Organisation, Department of Space, Government of India. S. J. Conway, M. Massé, and N. Mangold are supported by the French Space Agency, CNES. All the HiRISE image data used in this study are available via the PDS node (http://ode.rsl.wustl.edu/mars/). All boulder track data relevant to the morphometric results of this study are available in Data Set S1 (hosted at https://doi.org/10.6084/m9.figshare.13083992.v1). We thank NASA/JPL/University of Arizona for collecting and processing all the HiRISE images used in the study. Thanks to Jay Dickson and the Caltech Bruce Murray Laboratory for Planetary Visualization (http://murray-lab.caltech.edu/Mars2020/) for producing the global CTX mosaic and HiRISE digital elevation models used in the study.

References

Atwood-Stone, C., & McEwen, A. S. (2013). Avalanche slope angles in low-gravity environments from active Martian sand dunes. Geophysical Research Letters, 40(12), 2929-2934.

Banerdt, W. B., Smrekar, S. E., Banfield, D., Giardini, D., Golombek, M., Johnson, C. L., Lognonné, P., Spiga, A., Spohn, T., Perrin, C. and Stähler, S.C. (2020), Initial results from the InSight mission on Mars. Nature Geoscience, 1-7.

Beyer, R.A. (2012) Disappearing boulder tracks. http://www.uahirise.org/ESP_026055_1985

Brown, J. R., & Roberts, G. P. (2019), Possible evidence for variation in magnitude for marsquakes from fallen boulder populations, Grjota Valles, Mars. Journal of Geophysical Research: Planets, 124(3), 801-822.

Carrozzo, F. G., Bellucci, G., Altieri, F., D'aversa, E., &Bibring, J. P. (2009). Mapping of water frost and ice at low latitudes on Mars. Icarus, 203(2), 406-420.

Chojnacki, M., Banks, M., &Urso, A. (2018), Wind-driven erosion and exposure potential at Mars 2020 rover candidate-landing sites. Journal of Geophysical Research: Planets, 123(2), 468-488.

Cockell et al., Habitability: A review, Astrobiology, 16 (1), 89-117.

Copons, R., Vilaplana, J. M., & Linares, R. (2009). Rockfall travel distance analysis by using empirical models (Sola d'Andorra la Vella, Central Pyrenees). Natural Hazards & Earth System Sciences, 9(6).

Daubar, I. J., McEwen, A. S., Byrne, S., Kennedy, M. R., & Ivanov, B. (2013), The current martian cratering rate. Icarus, 225(1), 506-516.

Daubar, I. J., Banks, M. E., Schmerr, N. C., &Golombek, M. P. (2019), Recently Formed Crater Clusters on Mars. Journal of Geophysical Research: Planets, 124(4), 958-969.

Day, M., & Dorn, T. (2019), Wind in Jezero crater, Mars. Geophysical Research Letters, 46(6), 3099-3107.

de la Torre Juárez, M., Rodríguez Manfredi, J. A., Apéstigue, V., Arruego Rodríguez, I., Banfield, D. J., Boland, J. S. Boland, P. G. Conrad, R. Ferrándiz, E.Fischer,M. Genzer, J.Gómez-Elvira.

(2020). Performance of the MEDA Environmental and Meteorological Package for Mars 2020 After Integration. LPI, (2326), 2971.

Dickson, J. L., Kerber, L. A., Fassett, C. I., &Ehlmann, B. L. (2018, March), A global, blended CTX mosaic of Mars with vectorized seam mapping: a new mosaicking pipeline using principles of non-destructive image editing. In Lunar and Planetary Science Conference (Vol. 49, pp. 1-2).

Dundar, M., Ehlmann, B. L., &Leask, E. K. (2019), Machine-Learning-Driven New Geologic Discoveries at Mars Rover Landing Sites: Jezero and NE Syrtis. arXiv preprint arXiv:1909.02387.

Duszyński, F., Migoń, P., & Strzelecki, M. C. (2015). The origin of sandstone boulder aprons along the escarpments of the Stołowe Mountains: are they all rockfall-derived? A new insight into an old problem using the CONEFALL 1.0 software. Bulletin of Geography. Physical Geography Series, 8(1), 19-32.

Eppes, M. C., Willis, A., Molaro, J., Abernathy, S., & Zhou, B. (2015). Cracks in Martian boulders exhibit preferred orientations that point to solar-induced thermal stress. Nature communications, 6(1), 1-11.

Evans, S. G., &Hungr, O. (1993). The assessment of rockfall hazard at the base of talus slopes. Canadian geotechnical journal, 30(4), 620-636.

Farley, K., Morgan, K.S., &Williford, K. (2018), Jezero-Midway interellipse traverse mission concept, Fourth Landing Site Selection Workshop for Mars 2020, October 18, 2018.

Fassett, C. I., & Head III, J. W. (2005). Fluvial sedimentary deposits on Mars: Ancient deltas in a crater lake in the Nili Fossae region. Geophysical Research Letters, 32(14).

Golombek, M., & Rapp, D. (1997). Size-frequency distributions of rocks on Mars and Earth analog sites: Implications for future landed missions. Journal of Geophysical Research: Planets, 102(E2), 4117-4129.

Golombek, M. P., Haldemann, A. F. C., Forsberg-Taylor, N. K., Dimaggio, E. N., Schroeder, R. D., Jakosky, B. M., Mellon, M.T. and Matijevic, J.R. (2003). Rock size-frequency distributions on Mars and implications for Mars Exploration Rover landing safety and operations. Journal of Geophysical Research: Planets, 108(E12).

Golombek, M. P., Huertas, A., Marlow, J., McGrane, B., Klein, C., Martinez, M., M., Arvidson, R.E., Heet, T., Barry, L., Seelos, K. and Adams, D. (2008). Size-frequency distributions of rocks on the northern plains of Mars with special reference to Phoenix landing surfaces. Journal of Geophysical Research: Planets, 113(E3).

Golombek, M., Huertas, A., Kipp, D., &Calef, F. (2012). Detection and characterization of rocks and rock size-frequency distributions at the final four Mars Science Laboratory landing sites. IJMSE, 7, 1-22.

Goudge, T. A., Mustard, J. F., Head, J. W., Fassett, C. I., & Wiseman, S. M. (2015). Assessing the mineralogy of the watershed and fan deposits of the Jezero crater paleolake system, Mars. Journal of Geophysical Research: Planets, 120(4), 775-808.

Goudge, T. A., Milliken, R. E., Head, J. W., Mustard, J. F., &Fassett, C. I. (2017). Sedimentological evidence for a deltaic origin of the western fan deposit in Jezero crater, Mars and implications for future exploration. Earth and Planetary Science Letters, 458, 357-365.

Goudge, T. A., Mohrig, D., Cardenas, B. T., Hughes, C. M., &Fassett, C. I. (2018). Stratigraphy and paleohydrology of delta channel deposits, Jezero crater, Mars. Icarus, 301, 58-75.

Gupta, S. &Horgan, B. (2018), Mars 2020 Science Team Assessment of Jezero crater. In Mars 2020 4th Landing Site Workshop, October 16-18, 2018.

Hamilton, V. E., & Ruff, S. W. (2012). Distribution and characteristics of Adirondack-class basalt as observed by Mini-TES in Gusev crater, Mars and its possible volcanic source. Icarus, 218(2), 917-949.

Kleinhans, M. G., Markies, H., De Vet, S. J., &Postema, F. N. (2011). Static and dynamic angles of repose in loose granular materials under reduced gravity. Journal of Geophysical Research: Planets, 116(E11).

Kneissl, T., van Gasselt, S., &Neukum, G. (2011), Map-projection-independent crater size-frequency determination in GIS environments—New software tool for ArcGIS. Planetary and Space Science, 59(11-12), 1243-1254.

Kumar, P. S., Krishna, N., Lakshmi, K. P., Raghukanth, S. T. G., Dhabu, A., &Platz, T. (2019), Recent seismicity in Valles Marineris, Mars: Insights from young faults, landslides, boulder falls and possible mud volcanoes. Earth and Planetary Science Letters, 505, 51-64.

Landis, G. A. (2007). Observation of frost at the equator of Mars by the Opportunity rover. LPI, (1338), 2423.

Lied, K. (1977). Rockfall problems in Norway. ISMES Publication, 90, 51-53.

Malin, M. C., &Edgett, K. S. (2001), Mars global surveyor Mars orbiter camera: interplanetary cruise through primary mission. Journal of Geophysical Research: Planets, 106(E10), 23429-23570.

Mangold, N., G. Dromart, V. Ansan, M. Massé, F. Salese, M. Kleinhans, 2020, Fluvial Regimes, Age and Duration of Jezero Crater Paleolake and its Significance for the 2020 Rover Mission Landing Site, Astrobiology, https://doi.org/10.1089/ast.2019.2132.

McEwen, A. S., Eliason, E. M., Bergstrom, J. W., Bridges, N. T., Hansen, C. J., Delamere, W. A., Grant, J.A., Gulick, V.C., Herkenhoff, K.E., Keszthelyi, L. and Kirk, R.L. (2007), Mars reconnaissance orbiter's high resolution imaging science experiment (HiRISE). Journal of Geophysical Research: Planets, 112(E5).

Mellon, M. T. (1997). Small-scale polygonal features on Mars: Seasonal thermal contraction cracks in permafrost. Journal of Geophysical Research: Planets, 102(E11), 25617-25628.

Morris, R. V., Golden, D. C., Bell III, J. F., Shelfer, T. D., Scheinost, A. C., Hinman, N. W., Furniss, G., Mertzman, S.A., Bishop, J.L., Ming, D.W. and Allen, C.C. (2000). Mineralogy, composition, and alteration of Mars Pathfinder rocks and soils: Evidence from multispectral, elemental, and magnetic data on terrestrial analogue, SNC meteorite, and Pathfinder samples. Journal of Geophysical Research: Planets, 105(E1), 1757-1817.

Pajola, M., Lucchetti, A., Fulle, M., Mottola, S., Hamm, M., Da Deppo, V., Penasa, L., Kovacs, G., Massironi, M., Shi, X. and Tubiana, C. (2017), The pebbles/boulders size distributions on Sais: Rosetta’s final landing site on comet 67P/Churyumov–Gerasimenko. Monthly Notices of the Royal Astronomical Society, 469(Suppl_2), S636-S645.

Rice M. S., et al. The MastcamZ filter set and plans for multispectral imaging with Mars-2020 at Jezero crater, 51th LPSC, Houston, 2020.

Russell, P. S., et al. RIMFAX ground penetrating radar field tests in the Western USA, 51th LPSC, Houston, 2020.

Roberts, G. P., Matthews, B., Bristow, C., Guerrieri, L., &Vetterlein, J. (2012), Possible evidence of paleomarsquakes from fallen boulder populations, Cerberus Fossae, Mars. Journal of Geophysical Research: Planets, 117(E2).

Schmitt, H. H., &Cernan, E. A. (1973). A geological investigation of the Taurus-Littrow Valley.[characteristics of Apollo 17 flight lunar landing site].

Schon, S. C., Head, J. W., &Fassett, C. I. (2012). An overfilled lacustrine system and progradational delta in Jezero crater, Mars: Implications for Noachian climate. Planetary and Space Science, 67(1), 28-45.

Schorghofer, N., &Edgett, K. S. (2006). Seasonal surface frost at low latitudes on Mars. Icarus, 180(2), 321-334.

Senthil Kumar, P., Sruthi, U., Krishna, N., Lakshmi, K. J. P., Menon, R., Gopala Krishna, B., Kring, D.A., Head, J.W., Goswami, J.N. and Kiran Kumar, A.S. (2016), Recent shallow moonquake and impact-triggered boulder falls on the Moon: New insights from the Schrödinger basin. Journal of Geophysical Research: Planets, 121(2), 147-179.

Squyres, S. W., Arvidson, R. E., Bollen, D., Bell III, J. F., Brueckner, J., Cabrol, N. A., Calvin, W.M., Carr, M.H., Christensen, P.R., Clark, B.C. and Crumpler, L. (2006). Overview of the opportunity mars exploration rover mission to meridianiplanum: Eagle crater to purgatory ripple. Journal of Geophysical Research: Planets, 111(E12).

Stolper, E. M., Baker, M. B., Newcombe, M. E., Schmidt, M. E., Treiman, A. H., Cousin, A., Dyar, M.D., Fisk, M.R., Gellert, R., King, P.L. and Leshin, L. (2013). The petrochemistry of Jake_M: A Martian mugearite. science, 341(6153).

Tesson, P. A., Conway, S. J., Mangold, N., Ciazela, J., Lewis, S. R., &Mège, D. (2020), Evidence for thermal-stress-induced rockfalls on Mars impact crater slopes. Icarus, 113503.

Thomas, M. F., McEwen, A. S., & Dundas, C. M. (2019), Present-day mass wasting in sulfate-rich sediments in the equatorial regions of Mars. Icarus, 113566.

van der Bogert C.H., Plescia J.B. (2015), Boulder Track. In: Hargitai H., Kereszturi Á. (eds) Encyclopedia of Planetary Landforms. Springer, New York, NY.

Vincendon, M., Forget, F., & Mustard, J. (2010a). Water ice at low to midlatitudes on Mars. Journal of Geophysical Research: Planets, 115(E10).

Vincendon, M., Mustard, J., Forget, F., Kreslavsky, M., Spiga, A., Murchie, S., &Bibring, J. P. (2010). Near-tropical subsurface ice on Mars. Geophysical Research Letters, 37(1).

Wiens, R. C., Edgett, K. S., Stack, K. M., Dietrich, W. E., Bryk, A. B., Mangold, N., Bedford, C., Gasda, P., Fairen, A., Thompson, L. and Johnson, J. (2020). Origin and composition of three heterolithic boulder-and cobble-bearing deposits overlying the Murray and Stimson formations, Gale Crater, Mars. Icarus, 113897.

Williams, J., Day, M., Chojnacki, M., & Rice, M. (2020). Scarp orientation in regions of active aeolian erosion on Mars. Icarus, 335, 113384.